WARSAW UNIVERSITY OF TECHNOLOGY Index 351733
FACULTY OF CIVIL ENGINEERING
COMMITTEE FOR CIVIL AND WATER ENGINEERING
POLISH ACADEMY OF SCIENCES ISSN 1230-2945
DOI: 10.24425/ace.2025.155095
ARCHIVES OF CIVIL ENGINEERING
Vol. LXXI ISSUE 3 2025
pp. 217–230

© 2025. Guangqing Xiao, Xilong Chen, Lihai Xu, Fucheng Wu, Liang Zeng, Shaohua He.

This is an open-access article distributed under the terms of the Creative Commons Attribution-NonCommercial-NoDerivatives License (CC BY-NC-ND 4.0, https://creativecommons.org/licenses/by-nc-nd/4.0/), which permits use, distribution, and reproduction in any medium, provided that the Article is properly cited, the use is non-commercial, and no modifications or adaptations are made.

Research paper

Effective anchorage stress of prestressed tendons in PC girders under varying tensioning sequences

Guangqing Xiao[1], Xilong Chen[2], Lihai Xu[3], Fucheng Wu[4], Liang Zeng[5], Shaohua He[6]

Abstract: In current design codes, the standardized anchorage stress of prestressed tendons in concrete girders is uniform, which presents a notable challenge in accurately assessing the effective anchorage stress of girders with varying span lengths. This study investigates the impact of prestressed tendons' span length and tensioning sequences on effective anchorage stress in small-box girders (20 m, 25 m, 30 m) and 40 m T-shaped girders. Comprehensive theoretical approaches for computing the effective anchorage stress of the tendons, accounting for stress losses due to conduit friction, anchor deformation, rebar relaxation, concrete, and joint compression, are presented. The calculated results for prestressed concrete (PC) girders with typical span lengths and cross-sections demonstrate that girder length and tensioning sequence influence the effective anchorage stress of prestressed tendons. The currently recommended standardized effective anchorage stress of 1280 MPa in existing codes, derived solely from a designated length and anchorage retraction, proves inadequate for PC girders of varying lengths. Based on theoretical and numerical findings, refined effective anchorage stress of 1237 MPa, 1244 MPa, and 1251 MPa are proposed for small-box girders with span lengths of 20 m, 25 m, and 30 m, respectively, while the recommended effective anchorage stress for a T-shaped PC girder with a length of 40 m is 1251 MPa. Adoption of the evaluation method effective anchorage stress yields an improved prestressed quality passing rate ranging from 4.0% to 10.9%, thereby effectively reducing the necessity for unnecessary supplementary tensioning or excessive tensioning during on-site construction to meet project requirements.

Keywords: effective stress, finite element, prestress tendon, qualification rate, stress loss

[1]Eng., Guangzhou Guangjian Construction Engineering Testing Center Co., Ltd, Guangzhou 510405, China, e-mail: xiaogq2022@126.com, ORCID: 0009-0003-3978-6100
[2]Sen. Eng., Guangzhou Guangjian Construction Engineering Testing Center Co., Ltd, Guangzhou 510405, China, e-mail: 327991026@qq.com, ORCID: 0009-0008-9907-4590
[3]Eng., Guangzhou Guangjian Construction Engineering Testing Center Co., Ltd, Guangzhou 510405, China, e-mail: 1356583345@qq.com, ORCID: 0009-0003-3805-1196
[4]Sen. Eng., Guangzhou Guangjian Construction Engineering Testing Center Co., Ltd, Guangzhou 510405, China, e-mail: 2545504274@qq.com, ORCID: 0009-0008-0570-1857
[5]Eng., Guangzhou Guangjian Construction Engineering Testing Center Co., Ltd, Guangzhou 510405, China, e-mail: 18720836369@163.com, ORCID: 0009-0007-4329-6031
[6]Associate Professor, Guangdong University of Technology, Guangzhou 510006, China, e-mail: hesh@gdut.edu.cn, ORCID: 0000-0002-0727-1976

1. Introduction

The effective anchorage stress pertains to the residual tensile stress within the steel strand after the occurrence of prestress losses attributed to various contributing factors [1]. The effective anchorage stress of prestressed concrete (PC) girders significantly impacts bridge structural safety and serviceability [2–5], with improper reinforcement tension and inadequate anchorage stress potentially resulting in unexpected deflection, severe cracking, and non-uniform bridge alignment [6–9]. The absence of tailored evaluation standards may also lead to misguided construction practices, bringing safety matters during on-site tensioning operations. For example, tensioning of steel reinforcements based on standard parameters often yields minimal prestress results for 20 m and 25 m PC girders, making it challenging to meet evaluation criteria. To adhere to the standardized stress value of 1280 MPa, the super-tensioning method is commonly employed for 20 m and 25 m PC girders. However, this approach risks tendon breakage and flying anchor injuries and induces excessive arching in the midpoint, adversely affecting bridge alignment. Construction quality can be monitored throughout construction by conducting sampling inspections of effective anchorage stress under the anchor. However, the essential solution to address such issues is to establish rational evaluation criteria for standardizing tensioning practices, promptly identifying tensioning process issues, and implementing corrective measures.

In recent years, the assessment of effective anchorage stress under anchor has become widespread across numerous provinces in China. Per current standards and documents, the recommended standard value for effective anchorage stress under anchor stands at 1280 MPa. This value is derived analytically based on a single-tension detection principle using a 30 m precast small-box girder as the reference object. However, this calculation only accounts for stress loss due to anchorage retraction, neglecting the influence of elastic compression on effective anchorage stress varying girder length and sequential tensioning. In theory, given the same tension control force, the effective anchorage stress varies for prestressed tendons with different girder lengths and positions [10].

Numerous scholars have investigated the effective anchorage stress in PC bridges [11–17]. Based on the elastic wave theory, Chen et al. [9] proposed a rapid and efficient detection method for detecting prestress under prefabricated beam anchors. Dong et al. [10] analyzed the measured values of effective anchorage prestress in numerous PC bridges, emphasizing the importance of categorizing the measurement and control indices of effective anchorage prestress based on the tension length, distinguishing between lengths less than 20 m and those exceeding this threshold. Lin et al. [13] examined prestress loss in precast T-girders of varying lengths and proposed corresponding effective prestress loss rate ranges. Chen et al. [14] determined the critical structural safety state value and safety margin of effective prestress under anchor by analyzing T-girder mechanical properties under different tension levels. Based on anchor prestress test results, Yao et al. [15] identified issues in precast girder tensioning processes and enhanced prestress construction quality through tension parameter adjustments. Qing et al. [16] explored the time-dependent attenuation of prestress under anchor within a 48-hour tensioning period, revealing a logarithmic increase in measured prestress loss over time. As research angles diverge, scholars have begun focusing on evaluating effective prestress

under anchor. Chen et al. [17] compared evaluation outcomes of effective prestress under different control standards, finding that Control Standard 2, considering clip retraction and anchor ring anti-friction resistance, outperformed Control Standard 1, which only considered clip retraction, and Control Standard 3, referencing the "Chongqing Municipal Infrastructure Project Prestressed Construction Quality Acceptance Specification", offering more reasonable evaluation results. Overall, research on effective prestress under anchor primarily centers on prestress loss calculation and time-dependent prestress effects, with limited focus on evaluation standards for effective anchorage stress under anchor.

This paper investigates the impact of girder length and tensioning sequence on the effective anchorage stress through an integrated analysis of theoretical calculations, finite element simulations, and field measurements. The objective is to establish evaluation standard values for effective anchorage stress for small box girders of 20 m, 25 m, and 30 m lengths and for 40 m T-shaped girders. The study aims to standardize tensioning practices, mitigate the occurrence of unwarranted supplementary tensioning or excessive tensioning on prestressed construction sites, and offer practical guidance for engineering applications.

2. Computation formulas of prestressed effective anchorage stress

The effective prestress under the anchor is retained after the tension and anchorage of the steel tendon is retracted. The specification requires that the detection time be carried out within 24 hours after the anchorage, while the actual detection generally occurs within 5 hours after the anchorage. Generally, the stress loss in post-tensioned girders encompasses six parts: the stress loss arising from friction between prestressed tendons and the conduit (σ_{l1}), the stress loss due to anchorage compression and steel retraction (σ_{l2}), the stress loss caused by temperature disparities between prestressed tendons and concrete (σ_{l3}), the stress loss resulting from concrete compression (σ_{l4}), the stress relaxation of prestressed tendons (σ_{l5}), and finally, the stress loss associated with concrete shrinkage and creep (σ_{l6}) [18–20]. During the fabrication of a PC girder, the stress losses are primarily contributed by σ_{l1}, σ_{l2}, and σ_{l4}, as the remaining stress losses are contingent upon factors such as time and environmental conditions. Consequently, the effective stress beneath the anchor of the prestressed tendons, σ_{pe} can be accurately determined using the following equation:

$$\sigma_{\text{pe}} = \sigma_{\text{con}} - \sigma_{l1} - \sigma_{l2} - \sigma_{l4} \tag{2.1}$$

where: σ_{con} – the prestressing control stress of tendons (MPa).

Stress loss attributable to conduit friction is characterized by a progressive reduction in prestress as a result of the frictional forces between the prestressed tendons and the surrounding concrete or conduit, which intensifies with increasing distance from the tensioning end. This type of stress loss is intricately connected to a multitude of factors. Typically, several parameters must be quantified, encompassing the friction coefficient between the prestressed tendons and the conduit, the composite bending angle of the tendons, the deviation of the conduit, and the

length of the prestressed reinforcement extending from the anchoring end to the designated calculated section. According to the Chinese code [15], the quantification of σ_{l1} is achieved through the following mathematical expression:

$$\sigma_{l1} = \sigma_{\text{con}}[1 - e^{-(\mu\theta + kx)}] \tag{2.2}$$

where: μ – the friction coefficient between the prestressing tendon and the conduit, typically assumed to be 0.25, θ – the composite bending angle of the prestressed tendon, k – the coefficient quantifying the influence of conduit deviation per meter on friction, conventionally assumed to be 0.0015, x – the length of the prestressed tendon from the anchorage end to the calculated section.

After the final tensioning stage is completed, stress loss due to anchorage compression and steel retraction occurs. Specifically, the retraction of prestressed tendons comprises deformation induced by various factors, including anchorage deformation, reinforcement relaxation, and joint compression. Among these factors, reinforcement relaxation resulting from slipping the anchorage clamp is the primary contributor to tendon retraction. As tendons in PC girders are predominantly curved, the impact of reverse friction during the anchorage process on the anchorage retraction must be considered when determining the stress loss of σ_{l2}.

Figure 1 depicts the calculation diagram for σ_{l2}, accounting for the influence of reverse friction [21]. According to the Highway Bridge Specification [22], the friction coefficient exhibits a linear variation along the girder length, decreasing gradually from the tension end towards the mid-span point. Consequently, the effective stress in the prestressed tendons diminishes linearly from the anchorage to the mid-span. As shown in Fig. 1, the effective stress follows a three-point broken line pattern, marked as B, C, and D, due to the influence of reverse friction. The stress loss per meter, denoted as $\Delta\sigma_d$ resulting from the friction within the channel, can be accurately determined using Eq. (2.3).

$$\Delta\sigma_{l1} = \frac{\sigma_0 - \sigma_l}{l} \tag{2.3}$$

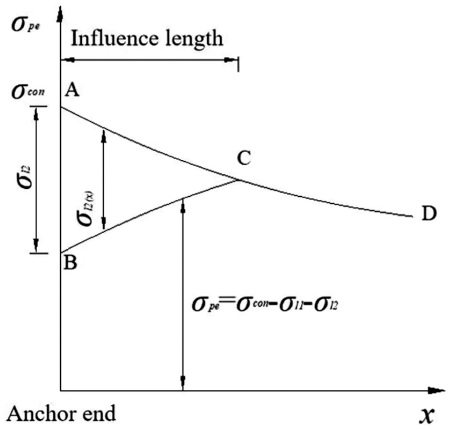

Fig. 1. Calculation diagram for stress loss considering reverse friction

where: σ_0 – the stress at the tension end (MPa), σ_l – the stress at the anchorage end (MPa), l – the distance from the tension end to the anchorage end (mm).

The reverse friction influence length, defined as l_f, can be determined using Eq. (2.4).

$$l_f = \sqrt{\frac{\sum \Delta l \cdot E_p}{\Delta\sigma_d}} \tag{2.4}$$

When $l_f \leq l$, the stress loss caused by anchorage retraction can be calculated using Eq. (2.5). When $l_f > l$, the anchorage retraction loss occurs in the full-length range of the prestressed tendon, and the stress loss caused by anchorage retraction can be calculated using Eq. (2.6).

$$\Delta\sigma = 2\Delta\sigma_d \cdot l_f \tag{2.5}$$

$$\Delta\sigma = \sum \Delta l \cdot \frac{E_p}{l_g} + \Delta\sigma_d \cdot l_g \tag{2.6}$$

The stress loss caused by concrete compression is produced during tensioning. The prestressed reinforcements are tensioned and anchored following a prescribed sequence, and the mechanism of stress loss caused by the concrete compression is plotted in Fig. 2.

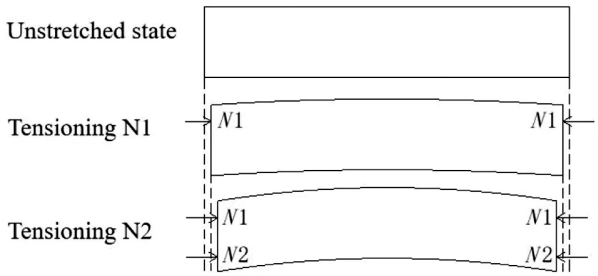

Fig. 2. Elastic compression mechanism diagram

The stress loss of σ_{l4} can be determined using the simplified calculation formula provided in the Chinese Highway Bridge Code [17], expressed as follows:

Utilizing Eq. (2.1) to (2.8), the effective anchorage stress of the prestressed tendons can be conveniently determined.

$$\sigma_{l4} = \frac{m-1}{2}\alpha_{E_P}\Delta\sigma_{pc} \tag{2.7}$$

$$\Delta\sigma_{pc} = \frac{N_p}{m}\left(\frac{1}{A_n} + \frac{e_{pn} \cdot y_i}{I_n}\right) \tag{2.8}$$

where: m – the number of prestressing tendons, α_{Ep} – the ratio of the elastic modulus of the prestressed tendon to the elastic modulus of concrete, $\alpha_{Ep} = E_p/E_c$, $\Delta\sigma_{pc}$ – the normal compressive stress of concrete produced by tensioning a tendon of reinforcements (MPa), N_p – the prestress of all tendons (deducting the prestress loss at the corresponding stage), A_n – the conversion cross-sectional area of the full cross-section of the member, I_n – the conversion cross-sectional moment of inertia of the full cross section of the member, e_{pn}, y_i – the distance between the center of gravity of prestressed tendons and the axis of the center of gravity of the converted section.

3. Calculation of effective anchorage stress of PC girders

In the widely disseminated diagram of prefabricated beams in China [23, 24], a comprehensive selection of simply supported PC girders is provided, encompassing distinct types such as the small-box girder and the T-shaped girder, both exhibiting varied spans, as depicted in Fig. 3. Among these, the PC girders most frequently employed include the small-box girder with span lengths of 20 m, 25 m, and 30 m, along with the T-shaped girder with a span length of 40 m. The girders are fabricated using C50 concrete with a target compressive strength of 50 MPa, Φ15.2 steel strand with a cross-sectional area of 139 mm^2, elastic modulus of 195 GPa, and ultimate tensile strength of 1860 MPa. The determinable tensile stress under the anchor is 1395 MPa.

As shown in Fig. 3, the tensioning sequence for the 20 m small box girder is N1 → N3 → N2 → N4, while for the 25 m and 30 m small box girders, it is N1 → N3 → N2 → N5 → N4. In the case of the 40 m T-shaped girder, the tensioning sequence is N2 → N5 → N1 → N3 → N4. Considering the steel strands are symmetrically tensioned at both ends, half of the girder length is considered the research object. Table 1 presents the composite bending angle and prestressed tendon length for the 20 m, 25 m, and 30 m small box girders and the 40 m T-shaped girder.

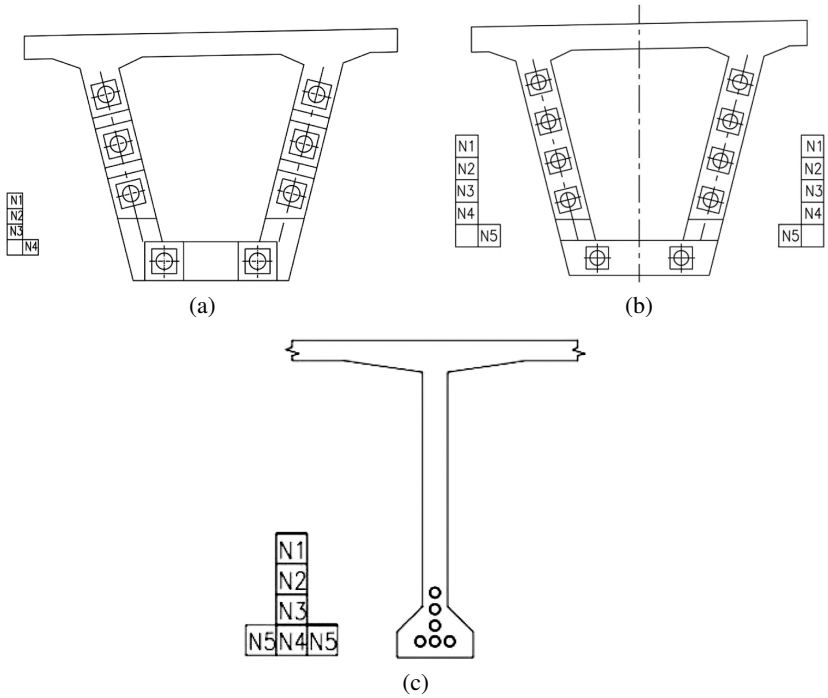

Fig. 3. Prestressed steel tendon tension sequence diagram: (a) 20 m small box girder, (b) 25 m and 30 m small box girder, (c) 40 m T-shaped girder

Utilizing Eq. (2.1) and the parameters specified in Table 1, the calculation of prestress friction loss at mid-span can be performed, and the results are presented in Table 2.

Table 1. Calculation parameters

Length of main girder (m)	Composite bending angle (°)					Length of steel strand (m)				
	N1	N2	N3	N4	N5	N1	N2	N3	N4	N5
20	5.3	5.3	5.3	2	–	9.83	9.82	9.81	9.80	–
25	5.3	5.3	5.3	5.3	2	12.33	12.32	12.32	12.30	12.30
30	5.3	5.3	5.3	5.3	2	14.84	14.83	14.83	14.82	14.80
40	7	7	7	7	6.5	19.65	19.64	19.63	19.61	19.60

Table 2. Prestressed duct friction loss

Length of main girder (m)	Duct friction loss σ_{l1} (MPa)				
	N1	N2	N3	N4	N5
20	51.84	51.82	51.80	32.30	–
25	56.87	56.85	56.85	56.81	37.40
30	61.90	61.88	61.88	61.86	42.48
40	81.25	81.23	81.21	81.18	78.28

According to many test results, the retraction of the anchorage is between 5.1 mm to 5.3 mm. Based on the principle of the most unfavorable conditions [13], the retraction value is defined as 5.3 mm. Subsequently, the length of the anti-friction effect of the anchorage shrinkage of the pre-stressed tendon is calculated. Then, the loss value of the anchorage shrinkage of the prestressed tendon is calculated according to Eq. (2.5). The results are shown in Table 3 and Table 4.

The anchored prestressed steel tendons should be tensioned in batches according to the prescribed sequence for small-box and T-shaped girders. The elastic deformation caused by the post-tensioned steel tendons will result in the prestressed loss of the pre-tensioned steel tendons. Combined with Eq. (2.6), the elastic compression loss value can be calculated, as shown in Table 5.

As tabulated in Table 6, the required effective anchorage stress can be determined using Eq. (2.8). for prefabricated girders of identical length, the effective anchorage stress exhibits variability depending on the positioning of steel tendon anchors and is influenced by the tensioning sequence, where later sequences correlate with higher prestress values. The final tensioned steel tendons for all girder lengths, denoted as N4, exhibit the highest anchorage stress. Additionally, a proportional relationship emerges between the average anchorage stress of the steel tendon section and girder length, indicating that longer girders yield greater average stresses. Post-tensioning of the entire section reveals average stresses of 1236 MPa, 1246 MPa,

Table 3. The influence length of prestressed anti-friction under anchor

Length of main girder (m)	**Anti-friction influence length (m)**				
	N1	**N2**	**N3**	**N4**	**N5**
20	14.00	13.99	13.99	17.71	–
25	14.97	14.97	14.97	14.96	18.44
30	15.74	15.74	15.74	15.74	18.98
40	15.81	15.81	15.80	15.80	16.08

Table 4. Prestressed anchorage retraction loss under anchor

Length of main girder (m)	**Retraction loss σ_{l2} (MPa)**				
	N1	**N2**	**N3**	**N4**	**N5**
20	156.98	157.05	157.12	137.77	–
25	140.72	140.72	140.72	140.86	121.44
30	131.51	131.58	131.58	131.58	112.30
40	130.79	130.79	130.79	130.79	128.49

Table 5. Prestress elastic compression loss under anchor

Length of main girder (m)	**Elastic compression loss σ_{l4} (MPa)**				
	N1	**N2**	**N3**	**N4**	**N5**
20	34.03	11.37	22.66	0.00	–
25	44.68	22.37	33.53	0.00	11.15
30	52.66	26.33	39.50	0.00	13.17
40	21.87	43.81	10.94	0.00	32.88

and 1251 MPa for the 20 m, 25 m, and 30 m small box girders, respectively, while the 40 m T-shaped girder exhibits an average stress of 1252 MPa. However, in routine prestress monitoring, code specifications typically mandate that for post-tensioned girders with a tension control stress of $0.75 f_{pk}$ and lengths exceeding 16 m, the stress must be evaluated against a standard value of 1280 MPa. As observed in Table 6, all tensioned steel tendon stresses and average section stresses, except for the anchorage stress beneath the anchor, deviate significantly from this benchmark, suggesting that the standard value of 1280 MPa may not be universally applicable to prestressing tendons with diverse girder lengths and tensioning sequences.

Table 6. Effective anchorage stress value under anchor

Girder length (m)	Effective anchorage stress under anchor (MPa)					Average value (MPa)
	N1	N2	N3	N4	N5	section
20	1214.03	1236.62	1225.18	1267.27	–	1214.03
25	1219.64	1241.94	1230.79	1264.17	1272.45	1219.64
30	1220.79	1247.12	1233.96	1273.45	1279.57	1220.79
40	1252.37	1230.43	1263.31	1274.24	1243.67	1252.37

4. Finite element analysis of prestress loss under anchor

The tensioning process of prestressed steel tendons often proceeds sequentially, with the prestress imparted to post-tensioned tendons potentially inducing compression or arching within the precast girder, thereby diminishing the prestress in the anchored steel tendons. To elucidate the impact of this tensioning sequence on the anchorage stress of steel bundles situated at varying positions, a simulation study was conducted. This analysis encompassed 20 m, 25 m, and 30 m standard small box girders, as well as 40 m standard T-shaped girders. The simulation methodology involved defining the construction stages in accordance with the tensioning sequence and employing compression elastic connections that aptly represent the tensioning pedestal. Furthermore, a realistic construction process was modeled, encompassing the grouting step after the tensioning of each full-section steel tendon.

Figure 4 shows the gradual change of anchorage stress under each anchorage point of the steel tendon with the order of tension.

The results presented in Fig. 4 demonstrate that:

(i) Upon tensioning, the effective anchorage stress exhibits distinct ranges for different girder lengths. Specifically, for the 20 m small box girder, the stress ranges from 1202.2 to 1235.3 MPa, averaging 1223.7 MPa. Similarly, for the 25 m, 30 m, and 40 m T-shaped girders, the ranges are 1223 to 1263.3 MPa (average of 1243.9 MPa), 1230.9 to 1269.1 MPa (average of 1248.2 MPa), and 1242.4 to 1277.0 MPa (average of 1259.7 MPa) respectively. A comparative analysis of the average anchorage stress values obtained through finite element analysis and theoretical calculations reveals a high degree of simulation accuracy, with the simulated values closely aligning with the theoretical predictions;

(ii) Among prefabricated girders of identical length, a distinct pattern emerges with regard to the influence of tensioning sequence on effective anchorage stress. Specifically, earlier tensioning of prestressed steel tendons results in a higher stress beneath the anchor, while the final tendons experience the lowest stress. This suggests that post-tensioned steel tendons incur greater prestress loss under the anchor compared to pre-tensioned tendons.

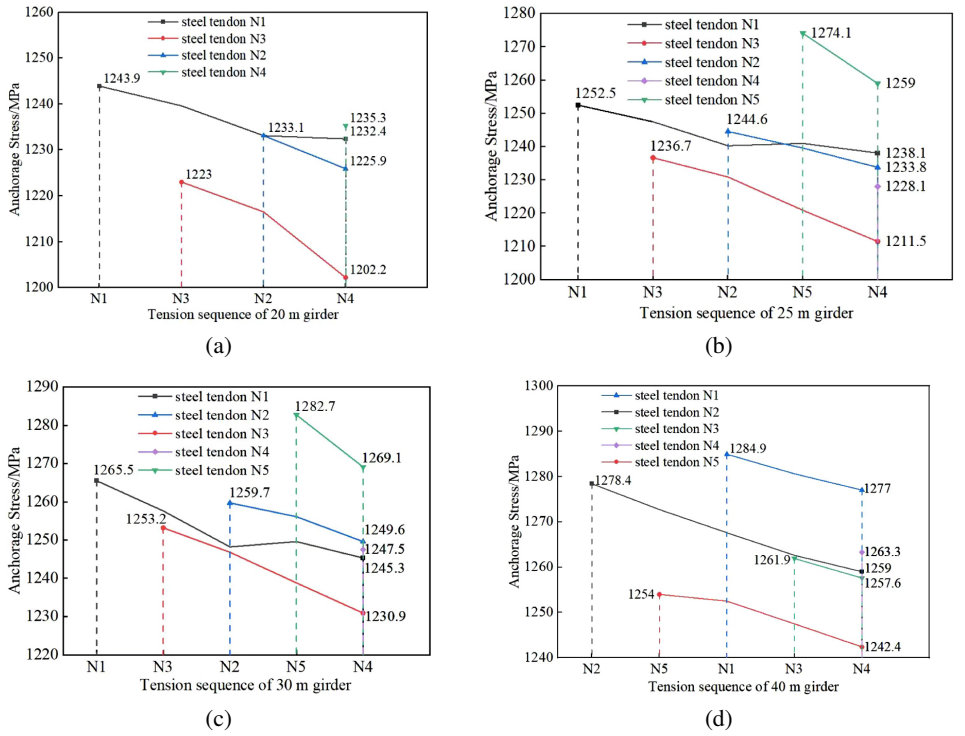

Fig. 4. Curve of effective prestress under anchor changing with tension sequence: (a) 20 m small box girder, (b) 25 m small box girder, (c) 30 m small box girder, (d) 40 m T-shaped girder

5. Statistical analysis of measured data of anchorage stress

To comprehensively evaluate the tension quality of prestressed steel tendons in a similar range of precast girder types, this study focuses on 20 m, 25 m, and 30 m small box girders as well as 40 m T-shaped girders, which are prevalent in engineering applications and have a significant number of test samples. By consolidating and categorizing the test results of effective anchorage stress of prestressed steel tendons available in this region, the presented analysis offers a macro-level perspective on their performance. The statistical outcomes of the anchorage stress are depicted in Fig. 5.

Figure 5 illustrates that, following the removal of individual outliers, the average stress values of the effective anchorage stress under the anchor for 20 m, 25 m, 30 m small box girder, and 40 m T-shaped girder are 1246.0 MPa, 1256.8 MPa, 1264.7 MPa and 1245.3 MPa respectively. The error range between the statistical value and the theoretical average falls within ±1.1%. Consequently, under normal circumstances, precast girders will need to be over-tensioned to a certain extent to meet the standard value of effective anchorage stress under the anchor at 1280 MPa.

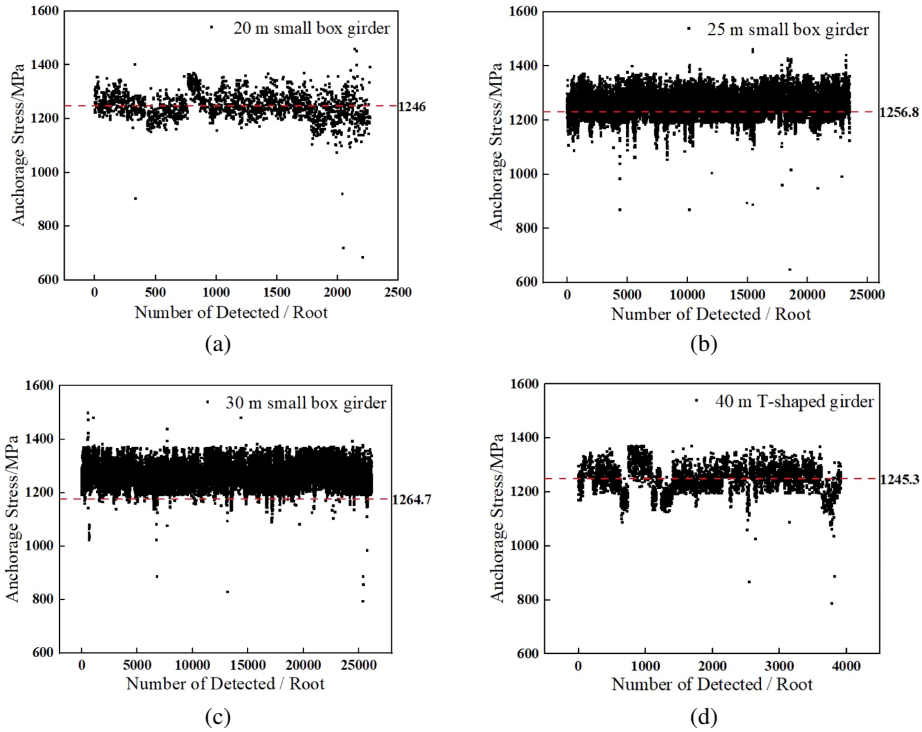

Fig. 5. Statistics of anchorage stress under anchor: (a) 20 m small box girder, (b) 25 m small box girder, (c) 30 m small box girder, (d) 40 m T-shaped girder

6. Qualified rate statistics assessment

Previous research has indicated that Li et al.'s [25] method for evaluating prestress under anchor considers the influence of frictional loss, anchor deformation, and rebar shrinkage on prestress loss. The predicted value obtained by this method is close to the standard value of 1280 MPa. However, this approach may lead to distorted evaluations when applied to anchorage prestress in PC beams of varying lengths and tension sequences. The analysis presented herein identifies two key limitations in the specification's stipulation of a standard value of 1280 MPa for effective anchorage stress. Firstly, it fails to account for the influence of girder length and tension sequence of steel tendons on prestress loss under anchor, resulting in significant discrepancies between calculated and actual effective anchorage stress. Secondly, for 20 m small box girders, the alignment of N1 and N3 steel tendon stress values with the average stress of the entire section is inadequate. Consequently, to fulfill evaluation criteria, construction sites resort to super-tensioning, posing substantial safety risks and potential economic losses.

To mitigate this issue, this study incorporates theoretical calculations, finite element analysis, and statistical analysis of measured data to determine the effective anchorage stress under the anchor for 20 m, 25 m, and 30 m small box girders, as well as a 40 m T-shaped girder. The predicted values are 1237.1 MPa, 1244.6 MPa, 1251.8 MPa, and 1251.8 MPa respectively, with a deviation from field measurements not exceeding 1.0%. To meet the required stress

levels, the anchorage stress under the anchor for 20 m, 25 m, 30 m small box girders, and 40 m T-shaped girder would need to be increased by 3.5%, 2.9%, 2.3%, and 2.3% compared to the standard value of 1280 MPa stipulated in the specifications. However, considering the 3% loss rate at the anchor ring as specified in highway bridge and culvert regulations [17], the resulting tensile coefficient would exceed the permissible limit of 105%, thus failing to satisfy the specifications for precast girders of varying lengths.

In the assessment of effective anchorage stress in prestressed steel tendon anchors, the conventionally specified qualified rate is typically maintained within a ±6% range. Nevertheless, given the influence of diverse girder lengths and tendon tensioning sequences, a more appropriate empirical value for effective anchorage stress can be derived. As demonstrated in Table 7, a comparative analysis reveals the predicted effective anchorage stress alongside the standard value of 1280 MPa stipulated in the specifications, highlighting the deviations from the qualified detection force rate.

Table 7. Statistics of the qualified rate of the standard and the evaluation method values

Value	**Qualified rate**			
	20 m	**25 m**	**30 m**	**40 m**
Standard	77.4%	86.9%	86.8%	75.1%
Evaluation Method	87.0%	90.9%	91.6%	86.0%

According to Table 7, the adoption of the proposed evaluation method to determine the standard value of anchorage stress under anchor led to significant improvements in the qualified rates of test results. Specifically, for 20 m, 25 m, and 30 m small box girders, the qualified rates were 87.0%, 90.9%, and 91.6% respectively, while for the 40 m T-shaped girder, it was 86.0%. Compared to the standard values stipulated in the specification, the evaluation standard resulted in notable enhancements, with increases in the qualified rates of 9.6%, 4.0%, 4.8%, and 10.9% for 20 m, 25 m, 30 m small box girders, and 40 m T-shaped girders, respectively.

The variance in standard values becomes more significant in the qualification rate of test results for priority tensioning prestressed tendons. Finite element analysis reveals that the anchorage stress at the anchor of steel tendon N3 in 20 m and 25 m small box girders, following sequential tensioning, is 1251.8 MPa and 1202.2 MPa, respectively. However, the lower limit of the interval determined by a 6% qualified rate of test results is 1211.5 MPa. Given the non-uniformity of the same prestressed steel tendon, the N3 stress value often fails to meet requirements. When evaluating with standard anchorage stress values of 1203.6 MPa and 1237.4 MPa, the respective lower limits are 1163.3 MPa and 1169.8 MPa, suggesting considerable room for improvement in prestressed tendon detection qualification rates. While girder length and tension sequence have limited impact on effective anchorage stress, they significantly influence test and evaluation outcomes.

Given the practical constraints of time and financial resources, the scope of this study is limited to the examination of the effective anchor prestress of simple supported beams. Future research may consider broadening the investigation to encompass a wider array of bridge structures, including those with continuous girder configurations.

7. Conclusions

This paper investigates the impact of girder length and tension sequence on effective anchorage stress of PC girders, and the following conclusions can be drawn from the present study:

1. The girder length and tensioning sequence critically influence the effective anchorage stress beneath the anchor, where the elastic compression of post-tensioned steel tendons contributes to prestress loss in pre-tensioned tendons. Moreover, variable lengths of post-tensioned tendons induce differing degrees of anchorage retraction loss, rendering the specified standard value of 1280 MPa, considering only single girder length and anchorage retraction loss, inadequate for practical application.
2. Theoretical and finite element analyses reveal consistent average prestressed section values beneath anchors for girders of identical lengths. Standard values for 20 m, 25 m, 30 m small box girders, and 40 m T-shaped girders are rounded to 1237.4 MPa, 1244.6 MPa, 1251.8 MPa, and 1251.8 MPa, respectively, deviating $\leq \pm 1.0\%$ from field averages, offering guidance for on-site prestressed tendon tensioning.
3. Using 1280 MPa as the standard anchorage stress reference, 20 m, 25 m, and 30 m small box girders, and 40 m T-shaped girders, require over-tensioning by 3.5%, 2.9%, 2.3%, and 2.3%, respectively. With a 3% loss rate, the tension coefficient for these prefabricated girders exceeds the specified 105% limit, violating specification requirements. This highlights deficiencies in the unified 1280 MPa anchorage stress standard.
4. While girder length and tensioning sequence do not affect effective anchorage stress, they significantly influence testing and evaluation outcomes. The evaluation method improved anchorage stress detection by 9.6% for 20 m, 4.0% for 25 m, 4.8% for 30 m small box girders, and 10.9% for 40 m T-shaped girders. This mitigates malicious or excessive tensioning to meet construction standards.

Acknowledgements

The authors express their sincere gratitude for the financial support provided by the Science and Technology Project of Guangzhou, China (Grant # 2024A04J9888).

References

[1] China Association for Engineering Construction Standardization, *Technical Standards of Effective Prestress under Anchorage Tests for Highway Bridge*. China Association for Engineering Construction Standardization, 2020.

[2] D. Mao, et al., "Research on influence of prestress loss of long span PC continuous girder bridge", *Highway Engineering*, vol. 47, no. 2, pp. 26–31, 2022, doi:10.19782/j.cnki.1674-0610.2022.02.005.

[3] Y. Liu, et al., "Parametric study on web cracks of PC box-girder bridges", *Journal of China & Foreign Highway*, vol. 41, no. 5, pp. 116–119, 2021, doi:10.14048/j.issn.1671-2579.2021.05.025.

[4] S. He, et al., "Experimental study on bond performance of UHPC-to-NC interfaces: constitutive model and size effect", *Engineering Structures*, vol. 317, art. no. 118681, 2024, doi:10.1016/j.engstruct.2024.118681.

[5] S. He, et al., "Performance assessment of channel beam bridges with hollow track bed decks", *Structures*, vol. 61, no. 5, 2024, doi:10.1016/j.istruc.2024.105988.

[6] W. Cao, "Research on mid-span deflection and crack control of long-span continuous rigid frame bridge", M.A. thesis, Shijiazhuang Railway University, China, 2019.

[7] W. Zheng, et al., "Research on treatment countermeasures of mid-span deflection disease of long-span rigid frame bridge", *Journal of Highway and Transportation Research and Development*, vol. 15, no. 5, pp. 194–196, 2019.

[8] J. Wang, et al., "Seismic performance of horizontal swivel system of asymmetric continuous girder bridge", *Archives of Civil Engineering*, vol. 69, no. 1, pp. 287–306, 2023, doi:10.24425/ace.2023.144174.

[9] S. He, et al., "Cracking performance in the hogging moment region of HSS-UHPC continuous composite girder bridges", *Structures*, vol. 61, no. 6, 2024, doi:10.1016/j.istruc.2024.106081.

[10] C. Ren, et al., "Primary investigation for unevenness of effective prestress", *Technology of Highway and Transport*, vol. 31, no. 6, pp. 63–67, 2015, doi:10.13607/j.cnki.gljt.2015.06.015.

[11] J. Chen, "Research on detection method of prestressed elastic wave under precast beam anchor", M.A. thesis, Chongqing Jiaotong University, China, 2018.

[12] M. Dong, "Research on the measurement and control index of effective prestress under anchor based on reliability theory", M.A. thesis, Chongqing Jiaotong University, China, 2017.

[13] J. Lin, et al., "Study on the reasonable range of effective prestress loss rate under post-tensioned precast T-beam anchor", *Journal of Highway and Transportation Research and Development*, vol. 9, no. 7, pp. 196–198, 2013.

[14] C. Chen, et al., "Study on the safety surplus of the valid prestressed force under anchor", *Highway Engineering*, vol. 38, no. 3, pp. 53–56, 2013

[15] Z. Yao, et al., "Construction quality control of prestressed post tensioning method based on effective pre-stressed detection of anchor", *Journal of China & Foreign Highway*, vol. 40, no. 4, pp. 179–183, 2020, doi:10.14048/j.issn.1671-2579.2020.04.039.

[16] Q. Jiang, et al., "Study on time-varing attenuation effect of anchor prestress within 48 hours after tensioning of steel strands", *Journal of China & Foreign Highway*, vol. 40, no. 4, pp. 105–109, 2020, doi:10.14048/j.issn.1671-2579.2020.04.022.

[17] X. Chen, et al., "Evaluation on effective prestress in anchor based on different control driteria", *Journal of China & Foreign Highway*, vol. 41, no. 3, pp. 92–95, 2021, doi:10.14048/j.issn.1671-2579.2021.03.019.

[18] J. Ye, *Structural design principle*. People's Communications Press, 1997.

[19] J. Wang, et al., "Stability monitoring method of UHPC spherical hinge horizontal rotation system", *Archives of Civil Engineering*, vol. 68, no. 3, pp. 601–616, 2022, doi:10.24425/ace.2022.141905.

[20] Ministry of Transport of the People's Republic of China, *Code for Design of Highway Reinforced Concrete and Prestressed Concrete Bridges and Culverts*. Beijing: People's Traffic Press, 2018.

[21] Y. Zhang, et al., "Study of the loss of prestress of tendon in post-tensioned prestressed concrete beams", *Journal of China & Foreign Highway*, vol. 15, no. 2, pp. 76–78, 2002, doi:10.3321/j.issn:1001-7372.2002.02.019.

[22] Ministry of Transport of the People's Republic of China, *General Code for Highway Bridges and Culverts*. China Communications Press, 2020.

[23] Z. He, et al., *Chaoshan Ring Expressway (including Chaoshan Connection Line)*. CCCC Highway Consultants Co., Ltd, 2017.

[24] X. Zhang, et al., *Construction Drawing Design of Humen Second Bridge Project*. CCCC Highway Consultants Co., Ltd, 2013.

[25] T. Li, et al., "Research on effective stress control technology of precast small box girder", *Sichuan Cement*, no. 11, pp. 49–51, 2023.

Received: 2024-05-08, Revised: 2024-07-21